R. & M. No. 3580

R. & M. No. 3580

MINISTRY OF TECHNOLOGY

AERONAUTICAL RESEARCH COUNCIL
REPORTS AND MEMORANDA

# Numerical Calculations of the Properties of Axially Symmetric Arc Columns

By A. WELLS

LONDON: HER MAJESTY'S STATIONERY OFFICE
1969
PRICE 15s. 0d. NET

# Numerical Calculations of the Properties of Axially Symmetric Arc Columns

By A. WELLS

*Reports and Memoranda No. 3580*

*March, 1967*

*Summary.*

Numerical solutions of the energy-balance equation of an axially symmetrical uniform arc column are outlined and illustrated with results pertaining to a nitrogen plasma at atmospheric pressure.

Published data on the electrical conductivity, thermal conductivity and radiated power density of nitrogen plasmas have been reviewed. The data selected for subsequent calculations of arc properties are summarised in Table 1 and Figs. 2, 3 and 4. Reasons for selecting these data are discussed.

Using the selected data, temperature distributions ($T(r)$), are radii ($R$), arc currents ($I$) and radiation losses ($U$), are calculated for arc columns in which the axial temperature, $T_0$, and the voltage gradient, $E$, have been specified. Results are summarised by a series of graphical plots (Figs. 8, 9 and 10) of arc similarity parameters $I/ER^2$, $U/R^2$, $EI-U$, against the axial temperature, $T_0$.

The purpose of the calculations is to provide data for comparison with experimental measurements on magnetically propelled arcs.

LIST OF CONTENTS



*Replaces R.A.E. Tech. Report No. 67076—A.R.C. 29 301.

---

1. *Introduction.*

A detailed study of the axially-symmetrical uniform arc column was undertaken in conjunction with the general investigation at R.A.E. into the interaction between electric arcs, gas streams and magnetic fields. Experimental work was first limited to measurements of the macroscopic properties of megnetically propelled arcs, i.e. measurements of arc current, arc voltage, arc velocity and applied magnetic field, combined with photography of arc shapes[1,2,3]. Corresponding theoretical analysis used a simplified model of the arc column to predict the aerodynamic drag and heat transfer associated with the column[4,5]. The model of the arc used in these analyses was based on the concept of a uniform axially-symmetrical arc column which was impermeable to the gas through which the arc moved. But, as Lord and Broadbent[4] showed by their analyses, the heat transfer rates predicted using this model were at least an order of magnitude smaller than the heat-transfer rates inferred from experimental measurements.

In order to investigate this discrepancy further and, in particular, to see whether the use of axially-symmetrical arc column as a model for magnetically propelled arcs was even partially justifiable, a

spectroscopic study of magnetically propelled arcs was initiated. The ultimate aim of this investigation was to study temperature distributions within the moving arcs using both time-integrating and time-resolving spectroscopic techniques. Initially, however, peak temperatures and arc widths were to be measured.

Accordingly, the apparatus necessary for this investigation was designed and constructed.

At the same time, calculations of the properties of axially-symmetrical uniform arc columns were started. The aim of these calculations was at providing theoretical data in an appropriate form for comparison with experimental measurements. It is the results of these calculations that are reported here.

First, temperature distributions were calculated for uniform arc columns in which the peak temperature, $T_0$ and the voltage gradient, $E$, could be specified. It was reasoned that if $T_0$ and $E$ were selected to correspond to values which could be measured in magnetically propelled arc experiments, then temperature variations throughout the moving arc column (deduced from measured time variations of the spectrum line intensity) could be compared with temperature distributions in the axially-symmetrical uniform arc column.

Secondly, as discussed in Section 4.2 of this Report, arc widths, arc currents and radiated power losses were calculated for axially-symmetrical arc columns. These calculations therefore enable one to make further direct comparisons between theoretical axially-symmetrical uniform arc columns and experimental magnetically-propelled arc columns for which arc widths, arc currents and electric fields and peak temperatures have been measured.

In this Report, a numerical method for solving the energy-balance equation of the axially-symmetrical uniform arc column is described. It is shown that temperature distributions, arc currents, arc radii and arc radiation loss can all be computed provided the peak temperature and voltage gradient in the arc column can be specified. Accordingly, the properties of a nitrogen arc at atmospheric pressure have been investigated. Comparisons of available data on plasma transport and radiative properties for a nitrogen plasma at atmospheric pressure have been made and reasons given for selection of particular sets of data for use in subsequent calculations. Some sample temperature distributions are discussed in Section 4.1. In Section 4.2 the variations of arc properties (voltage gradient, current, radius, radiated power) with peak temperature are presented using a series of arc similarity parameters.

## 2. *The Energy Balance in the Arc Column.*

### 2.1. *The Energy-Balance Equation.*

In an arc column within which heat transfer by convective means is negligible, the energy dissipated in an elemental volume of an arc column is transferred to the region outside the arc either by thermal conduction or by radiation.

$$\sigma(T)E^2 - \nabla \cdot \underline{J} + \nabla \cdot K(T)\nabla T = 0 \tag{1}$$

where $\sigma(T)E^2$ is the energy dissipated per unit volume of arc plasma at temperature $T$

$\sigma(T)$ is the electrical conductivity of the plasma

$E$ is the applied electric field

$\nabla \cdot \underline{J}$ is the total energy lost by radiation from unit volume of the plasma at temperature $T$

$\underline{J}$ is the total radiation flux density

$\nabla \cdot K(T) \nabla T$ is the total energy lost by thermal conduction

$K(T)$ is the thermal conductivity of the plasma.

If it is assumed that the arc column is axially-symmetric with uniform properties along its length, only radial heat losses need be considered. Furthermore, if the plasma is optically thin, all energy radiated from within the plasma escapes without being re-absorbed within the plasma column. Then the energy balance equation simplifies to:

$$\sigma(T)E^2 - P(T) + \frac{1}{r}\frac{d}{dr}\left(r\,K(T)\frac{dT}{dr}\right) = 0 \tag{2}$$

where $P(T) = 1/r\; d/dr\,(r\,J_r)$ is the radiated energy per unit volume of plasma.

For the purposes of these calculations, it has been assumed that the heat passing through the boundary of the arc is taken away by some external agency which acts as a heat sink. This agency might be a convective gas flow or the cooled wall of a stabilizing tube. It is therefore assumed that the mechanism by which the heat sink absorbs the heat crossing the arc boundary has no influence on the heat transport mechanisms acting within the arc column. For this purpose, the arc boundary is defined by a temperature which is sufficiently low for the electrical conductivity of the gas to be negligible compared with that of the arc plasma.

The material functions of the arc plasma, $\sigma$, $K$ and $P$, are in general complicated functions of temperature, pressure and the arc gas. Consequently, solutions of equation (2) are best approached using a numerical method.

The alternative is to represent the material functions by approximate analytical functions of $T$ and $P$ and hence to solve equation (2) analytically. The latter approach has been used quite frequently to analyse experimental arc characteristics or to deduce similarity relationships for arcs. Typical applications of analytical methods are to be found in AGARDograph 74 (Lord[4], Marlotte[6]) which also contains a bibliography of related work. No further discussion of analytical solutions will be given here.

### 2.2. *A Numerical Method for Solution of the Energy Balance Equation.*

We consider unit length of the uniform arc column and divide the circular cross-section into a large number of concentric annuli of equal widths. Each annulus is assumed to contain arc plasma whose material properties, $\sigma$, $K$ and $P$ have coefficients which remain constant within the annulus. At the boundaries between adjacent annuli, coefficients of the material functions are assumed to change discontinuously. The coefficients allocated to each annulus are chosen so as to be appropriate to the temperature within the annulus.

With reference to Fig. 1, let us consider the $i^{\text{th}}$ annulus; that is, the annulus confined within the radii $r_{(i-1)}$ and $r_i$. Let $\sigma$, $K$ and $P$ have the values $\sigma_i$, $K_i$ and $P_i$ within the $i^{\text{th}}$ annulus and let the temperature at $r_{(i-1)}$ be $T_{(i-1)}$.

For $r_{(i-1)} \leqslant r \leqslant r_i$, from equation (2):

$$(\sigma_i E^2 - P_i) \int_{r_{(i-1)}}^{r} r\,dr = -K_i \int_{r_{(i-1)}}^{r} \frac{d}{dr}\left(r\frac{dT}{dr}\right)dr \tag{3}$$

integration of which gives:

$$\left(\frac{dT}{dr}\right)_r = T'_{(r)} = -A_i\left[T_{(i-1)}\right] r + \frac{B_i\left[T_{(i-1)}, T'_{(i-1)}\right]}{r} \tag{4}$$

where

$$A_i[T_{(i-1)}] = \frac{\sigma_i E^2 - P_i}{2K_i} \tag{4a}$$

and

$$B_i[T_{(i-1)}, T'_{(i-1)}] = A_i r^2_{(i-1)} + T'_{(i-1)} r_{(i-1)} \tag{4b}$$

$T'_{(i-1)}$ is the radial temperature gradient at $r_{(i-1)}$.

Integration of equation (4) gives the temperature distribution across the annulus in a form suitable for numerical evaluation from the centre, equation (5)

$$T = T_{(i-1)} - \frac{A_i}{2}[T_{(i-1)}](r^2 - r^2_{(i-1)}) + B_i[T_{(i-1)}, T'_{(i-1)}] \log_e\left(\frac{r}{r_{(i-1)}}\right) \tag{5}$$

with the end conditions $T(0) = T_0$ and $T'(0) = 0$.

Thus integration can be performed over the whole arc cross-section to provide the variation of the plasma temperature as a function of radius within the arc column.

Because the temperature varies between $T_{(i-1)}$ and $T_i$ across the $i^{th}$ annulus, the choice of coefficients for $\sigma_i$, $K_i$ and $P_i$ appropriate to the $i^{th}$ annulus is not entirely explicit. In order to facilitate the numerical calculations, values of $\sigma$, $K$ and $P$ were tabulated against temperature at frequent regular intervals of temperature, $\Delta T$. Once $T_{(i-1)}$ had been determined at $r_{(r-1)}$, the tabulated temperature closest to $T_{(i-1)}$ was selected and the corresponding values of $\sigma$, $K$ and $P$ were used in solving equation (2) in the $i^{th}$ annulus. For the actual calculations, the data for $\sigma$, $K$ and $P$ were tabulated at 250°K intervals from 5000°K up to 30 000°K.

As well as calculating the temperature variations across each annulus, it is also possible to determine the electrical power $\Delta W_i$ dissipated in the $i^{th}$ annulus and the radiated power loss, $\Delta U_i$ from the $i^{th}$ annulus per unit length of uniform arc column.

$$\Delta W_i = 2\pi \sigma_i E^2 \int_{r_{(i-1)}}^{r_i} r\, dr \tag{8a}$$

$$\Delta U_i = 2\pi P_i \int_{r_{(i-1)}}^{r_i} r\, dr\,. \tag{8b}$$

The total power input, $W$, and the total radiated power loss, $U$, from unit length of arc column are obtained by integrating equations (8) over the whole arc cross-section.

Simple repetitive calculations of the kind described above are readily accomplished using a digital electronic computer and an Autocode Programme has been prepared for use with the R.A.E. Mercury Machine.

3. *Material Properties of Arc Plasmas.*

3.1. *Sources of Data.*

Evidently, knowledge of the dependence on temperature of the material properties of the arc plasma (electrical conductivity, $\sigma$, thermal conductivity $K$ and radiated power density, $P$) is essential for satisfactory solution of the energy balance equation. These properties may be determined either by direct

reference to physical theory or by analysis of experimental measurements on electric arcs.

There are a number of examples of published work in which calculations of properties have been made from kinetic theory and statistical mechanics but considerable discrepancies exist between the various results obtained. The theory underlying these calculations has been briefly outlined in Appendix A in which methods of calculating electrical and thermal conductivities of arc plasmas from transport theory and radiated power densities from radiation theory are discussed.

Properties derived by various authors for a nitrogen plasma at atmospheric pressure have been surveyed and two of the more recent sets of data (King[7]* and Yos[8]) are summarised in Figs. 2, 3 and 4. Discrepancies between the results of these two authors are clearly illustrated. Also shown in Figs. 2, 3 and 4 are examples of the plasma properties deduced by analysis of experimentally determined characteristics of a wall stabilised nitrogen arc. As can be seen, the results obtained by different authors (Uhlenbusch[9] and Monterde-Garcia[10]) are not entirely consistent with one another. The methods of analyses are briefly outlined in Appendix B.

### 3.2. *Properties of a Nitrogen Plasma at Atmospheric Pressure for Use in Subsequent Calculations.*

It is not obvious just from inspection of Figs. 2, 3 and 4 whether any single set of data is in any way superior to any other set. However, greater emphasis has been placed on sets of data which are reasonably well corroborated by data derived from other independent sources. In addition, the magnitudes of collision cross-sections, radiative absorption coefficients and particle densities used in theoretical calculations of the plasma transport and radiative properties were compared, wherever possible, with the corresponding values of these quantities obtained from quantum mechanics and atomic physics. (The relationships between the transport and radiative properties of the plasma ($\sigma$, $K$ and $P$) and collision cross-sections, absorption coefficients and particle densities are described in Appendix A.)

The selection of data on electrical conductivity up to temperatures of about 16 000°K presented little difficulty because magnitudes of electron-atom collision cross-sections are reasonably well established. In fact, Uhlenbusch's experimentally derived data from 6000°K up to 16 000°K has been used here as this is well supported by King's and Yos's theoretical data. In this range of temperatures, the limits of reproducibility of the experimentally derived data encompass the spread in the theoretical data. At temperatures below 6000°K and above 16 000°K, King's more recent (unpublished) electrical conductivities have been used. The reasons for this choice are that Uhlenbusch's data merges reasonably well with King's data which in turn uses well substantiated electron collision cross-sections and up-to-date values of electron, ion and atomic densities ($N_e$, $N_i$, $N_o$) as calculated by Burhorn and Wienecke[11]. Nevertheless the divergence between King's and Yos's data (Fig. 2) above 15 000°K is disquieting. It is probably due to the different values assumed by these authors for the electron-ion collision cross-section.

Selection of the most appropriate thermal conductivity data is not altogether straightforward. The largest discrepancy between theoretical results of Yos and King (unpublished) lies in the temperature range from 10 000°K to 20 000°K (Fig. 3) corresponding to a strong dependence on temperature of the degree of ionization of the plasma. The discrepancies arise from the choice of collision cross-section of nitrogen ions interacting with neutral atoms. As this collision cross-section has never been measured in an independent experiment, the differences remain unaccounted for. However, the experimentally derived data[9,10] tend to indicate the existence of an ionization peak at 15 000°K thus supporting King's results. For this reason Uhlenbusch's data has again been selected for the temperature range from 6000°K up to 16 000°K and King's unpublished data has been used over the rest of the temperature range. The reproductibility of the experimentally deduced data varies in the range 6000°K – 16 000°K from $\pm 25$ per cent near the dissociation peak at 7000°K to $\pm 8$ per cent at 15 000°K. At 7000°K the spread embraces the complete range of variation between all available data but at 15 000°K both Yos's and King's unpublished

*In a private communication following publication of this Report, King has informed the author that he has recently revised his data on the thermal conductivity of nitrogen and obtained values in the temperature range 10 000°K to 15 000°K which are very similar to the values finally used in the calculations reported in this paper.

theoretical data fall outside the limits of reproducibility. At temperatures below 6000°K and above 16 000°K, King's unpublished data merge reasonably well with the Uhlenbusch data. However, no great reliability is attached to these data above about 20 000°K as many of the cross-sections used in the calculations are unsupported by experimental measurements.

Regarding the radiation data[8,9,10,12], there are wide discrepancies between all three sets of theoretical data. For reasons discussed in Appendix A.3, the data calculated by the author (modified Pelzer data) is considered to be the most realistic in that empirical factors in the formula (equation A.7) have been chosen such that the data agree with the experimentally derived data[9,10]. In the temperature range up to about 16 000°K the experimentally derived data and the modified Pelzer data agree very closely. The theoretical data can probably be used up to about 22 000°K with confidence. However, above 22 000°K, the contribution to the radiation due to recombination of electrons and doubly ionized nitrogen atoms begins to predominate. As the calculated radiated power densities take no account of the re-absorption processes and as much of the double ion recombination must occur at very short wavelengths—which are unlikely to escape unabsorbed from an arc column at atmospheric pressure—the theoretical radiation curve probably overestimates the true amount of radiation emitted by the arc.

It is thought that, within the temperature range from 5000°K to about 20 000°K, the maximum error in the data on plasma properties of an atmospheric nitrogen plasma used in the ensuing calculations is unlikely to exceed $\pm 50$ per cent of the values given in Figs. 2, 3 and 4 and in Table 1; over much of the range the accuracy is much better than this. However at temperatures above 20 000°K it is not really possible to estimate the accuracy of the data.

## 4. *Calculations of Arc Properties.*

Using the numerical method described in Section 2 and the data summarized in Table 1 (Section 3), temperature distributions, currents, power inputs and radiation losses were calculated for arcs in nitrogen at atmospheric pressure. In order to make these calculations axial temperatures, $T_o$ (°K), and electric fields, $E$, had to be specified and a temperature, $T_R$, corresponding to the temperature at the radial limit of the conducting arc column had also to be chosen. A value of $T_R = 5000$°K was selected initially as the temperature of the arc column periphery since the arc plasma has a very low electrical conductivity, ($\sigma = 5 \times 10^{-3}$ (ohm–cm)$^{-1}$) at this temperature. Subsequently, calculations were also made for a range of values of $T_R$ with a view to investigating the importance of the choice of $T_R$ on general arc properties.

The calculations fall into two groups using two variations of the basic computer programme. In the first group, complete temperature distributions were computed. These results were used initially to compare computed distributions with Maecker's[13] measured temperature distributions in wall stabilised arcs, and subsequently to compute temperature distributions for various other arc conditions. The results are summarised in Section 4.1. below.

In the second group, the total power input, the total radiation power loss, the current, and the arc radius were computed using a selection of peripheral temperatures $T_R$. These results are summarised in Section 4.2 below.

### 4.1. *Temperature Distributions in a Nitrogen Arc.*

4.1.1. *Temperature distributions obtained using different sources of plasma property data.* Comparisons were made between computed temperature distributions obtained using:

(i) King's[14] early published data on electrical and thermal conductivities (not shown in Figs. 2 and 3) together with Pelzer's[12] radiation data.

(ii) Yos's[8] published data for $\sigma$, $K$ and $P$.

(iii) The Table 1 data for $\sigma$, $K$ and $P$ used in all subsequent computations. These data are based on Uhlenbusch's[9] experimental data combined with King's[7] unpublished data as discussed in Section 3 and Appendices A and B.

Accordingly, temperature distributions were calculated for arcs with an axial temperature of 15 000°K sustained in a uniform column of 25·0 V/cm, using the three different sets of data. The resulting distributions are shown in Fig. 5. Also shown is the temperature distribution measured by Maecker in a wall

stabilised arc operated at 25 V/cm at 200 amps. In order to make a further comparison between the various sets of data, the arc current, the power radiated and the column radius at $T_R = 5000°K$ were also calculated, the results being shown in Table 2.

Both the temperature distributions in Fig. 5 and the currents and radii listed in Table 2 show that results obtained using the Table 1 data—(iii) above—agree most closely with Maecker's experimental results. However, it will be recalled that over the temperature range 6000°K to 16 000°K the Table 1 data was based on Uhlenbusch's data which itself was derived from Maecker's measurements. Therefore the agreement is merely a reflection of the accuracy of Uhlenbusch's derivations of the data combined with the accuracy of subsequent calculations of arc properties using this data.

However, the other results shown in Table 2 show that use of Yos's data leads to the arc size and current being underestimated in calculations of arc properties for a given axial temperature and electric field. These discrepancies are associated with Yos's low values of thermal conductivity at temperatures above 10 0000°K combined with his high radiation values. On the other hand use of the King/Pelzer data leads to the radiation loss and consequently the arc current and arc size being overestimated.

The results in Table 2 therefore show the Table 1 data to be more applicable for calculations of arc properties; at least up to temperatures of 15 000°K where meaningful comparisons with experimental measurements have been possible.

4.1.2. *Temperature distributions at constant arc input power.* Using the data given in Table 1, a number of temperature distributions were calculated for a range of axial temperatures and electric fields. Among these computations were a set in which the effects were investigated of changing the arc size at constant input power. This was achieved by contriving to adjust the axial temperature, $T_o$, and the column voltage gradient, $E$, such that the product of $E$ and the arc current remained constant. The resulting temperature distributions of three arc columns all sustaining an input power of 10 kilowatts/cm at four different voltage gradients (and hence different arc radii) are shown in Fig. 6. In Fig. 7a, the variations of axial temperature $T_o$ with voltage gradient, $E$, at constant power inputs of 5 kilowatts/cm and 10 kilowatts/cm are shown, together with in Fig. 7b the variation of the radiated power density with voltage gradient at the same constant power inputs.

In his analysis of the arc column, King[14] showed that when radiation from the arc column was neglected, the temperature distributions in the arc column appeared to be a function only of the product $Er$ (voltage gradient × radius) independent of the individual values of $E$. It then followed that the axial temperature in the column was also independent of $E$ at constant power input. The results in Figs. 6 and 7 show that when the radiation loss cannot be ignored, temperature distributions are no longer a function only of $Er$ and, at constant power input, the axial temperature depends on the voltage gradient.

The physical explanation is as follows. Within an elemental zone in the plasma at a given temperature, the energy dissipated by ohmic heating increases as $E^2$ whereas the power radiated is unchanged since $P$, like $\sigma$, depends only on the temperature at constant pressure. Of the total heat generated within the elemental zone a fraction $(1 - P/\sigma E^2)$ has to be conducted away and the larger the field, $E$, the steeper the temperature gradient has to be in order to sustain this conduction loss. Consequently, arcs sustaining higher fields have smaller radii. Therefore, the volume of plasma per unit length of arc column is less and the radiation loss is correspondingly smaller. It follows, therefore, that arcs running in wide channels are sustained by a lower voltage gradient and attain a lower axial temperature by virtue of the cooling effect of the radiation loss.

Fig. 7 shows that under conditions of constant power,

(i) the total radiation loss decreases with increasing $E$ reaching quite a low level at fields exceeding 30 volts/cm;

(ii) with increasing $E$, the axial temperature tends to become independent of $E$.

It is concluded that in arcs sustained by high electric fields, i.e. arcs in narrow channels, the radiation cooling effects are negligible and arc columns can be reasonably well represented by a radiation-neglected energy-balance theory[14]. However, at lower fields, corresponding to arcs in wider channels, radiation

losses profoundly affect the temperature distribution, and therefore all related properties of the arc, and cannot be neglected.

4.2. *Overall Arc Properties.*

4.2.1. *Formation and use of arc similarity parameters.* Lord[15] has applied the methods of dimensional analysis to arc columns and has shown that certain non-dimensional groups of arc variables have simple functional relationships with each other. From this analysis, three similarity parameters $I/ER^2$, $EI-U$, and $U/R^2$ have been selected and it can be shown that they are functions of the central temperature, $T_o$, of the arc column. These functions have been calculated from the numerical solutions of the energy-balance equation (equation (2)) for the arc column (Section 2) using the best available plasma property data for a nitrogen plasma at atmospheric pressure (Section 3). The calculations yield results which are illustrated in Figs. 8, 9 and 10 and discussed further in Section 4.2.2. They summarise the properties of any axially symmetrical arc column in nitrogen at atmospheric pressure with the appropriate peripheral temperature $T_R$.

These results are intended to provide a means of interpreting measurements made on magnetically propelled arcs. In particular, spectroscopic measurements of the central temperature and the width of radiating zones could be combined with the measured currents and electric fields[3] in certain magnetically propelled arcs. Then, it may be possible to deduce from the graphs in Fig. 8, a peripheral temperature for the arc and so define an inner arc core in which convection heat losses are negligible. Figs. 9 and 10 can then be used to determine the radiation loss from the arc column. Such results would be useful in stipulating the boundary conditions necessary for analysis of the flow around an arc column[20].

4.2.2. *Numerical calculations of functional relationships between similarity parameters and arc central temperature.* The arc radius for an assumed peripheral temperature of 5000°K was calculated for a range of conditions of axial temperature and column voltage gradient in the arc. The power input and radiated power loss per unit length of arc column were also obtained from these calculations. Then, magnitudes of the groups $I/ER^2$, $U/R^2$ and $EI-U$ were calculated from the results.

It was found that at any given axial temperature within the range 7500°K to 25 000°K, computed values of the group $I/ER^2$, $U/R^2$, $EI-U$ gave constant values independent of the individual values of the parameters $E$, $I$, $R$, $U$, to within limits of $\pm 1{\cdot}5$ per cent. As will be shown in Section 4.3, these limits lie within the accuracy of the numerical calculation. Thus the behaviour of the groups $I/ER^2$, $U/R^2$ and $EI-U$ as similarity parameters was confirmed.

The parameters themselves were then plotted against $T_o$, Figs. 8, 9 and 10.

The major uncertainty involved in the preparation of these graph lies in the choice of the peripheral temperature $T_R$ for which a value of 5000°K was initially chosen. To remove this uncertainty to some extent, the parameters $I/ER^2$, $U/R^2$ and $EI-U$ were recalculated for values of $T_R$ of 7000°K and 9000°K: also shown in Figs. 8 to 10.

As can be seen from Figs. 8 to 10, incorrect choice of a peripheral temperature $T_R$ does not greatly affect the magnitude of the similarity parameters of arcs with high central temperatures. For example, a change of $T_R$ from 5000°K to 9000°K brings about a change in $I/ER^2$ of less than 20 per cent; in $EI-U$ of less than 4 per cent; and in $U/R^2$ of less 24 per cent for all axial temperatures exceeding 15 000°K.

At axial temperatures below 15 000°K, variations in the choice of peripheral temperature have a somewhat larger influence on the magnitude of the similarity parameters. This is to be expected since in a low current arc with low $T_o$ less heat has to be conducted across the arc boundary so that the temperature gradient at a given temperature zone in the arc is correspondingly steep. Therefore, an increase in $T_R$ leads to a decrease in the effective arc radius $R$, and the decrease in $R$ is greater, the smaller the temperature gradient and the smaller the conduction heat loss.

In typical experiments with wall stabilised arcs, (with central temperatures of the order 15 000°K) voltage gradients can probably be measured to within $\pm 10$ per cent, arc currents can be stabilised, probably to within 5 per cent whilst the radiation might be measured to within 20 per cent. Thus it appears that values of $I/ER^2$ or $U/R^2$ obtained from even the most controlled experiments on arcs have about the same order of accuracy as the spread of these parameters due to assumed changes in $T_R$ over the range

from 5000°K to 9000°K. In other words, even of uncertainties in the choice of $T_R$ were very large, the universal curves Figs. 8 to 10 could still be used to predict properties of arcs for $T_o$ equal to or greater than 15 000°K to within the accuracy that one might expect from an experimental determination of the same properties.

In fact, for many purposes it is reasonable to assume a peripheral temperature of around 5000°K—the electrical conductivity being so small at this temperature as to be essentially negligible—and therefore to use the universal curves for $T_R = 5000$°K over the whole temperature range covered by Figs. 8 to 10.

4.3. *Accuracy of the Calculations.*

The results described in Sections 4.1 and 4.2 of this Report may be in error from any one of three possible causes:

(i) Incorrect plasma property data.

(ii) Incorrect choice of arc peripheral temperature.

(iii) Errors introduced by the use of a stepwise computational method.

(i) and (iii) above would affect all the results; (ii) would only affect the universal curves—Figs. 8 to 10.

The uncertainties in the arc plasma data have already been discussed in Section 3 and Appendices A and B. The effects of uncertainties in the data have been illustrated by the results discussed in Section 4.1.1 and summarised in Table 2. From the results shown in Fig. 5 it was apparent that very large errors in the temperature distribution would result from the use of inappropriate plasma data, whilst Table 2 shows that similar large errors would be introduced into calculations of current and radiation for the same reason. No other estimates of errors due to incorrect plasma data have been made, in connection with the calculations reported here.

The effects of uncertainties in the choice of the arc peripheral temperature have also been discussed at length in Section 4.2.2. As mentioned there, the error introduced in calculated similarity parameters as a results of large uncertainties in $T_R$ rarely exceeds uncertainties that one would expect in any experimental determination of the same quantity.

Errors arising from the numerical integration process have also been investigated. The errors are due to dividing the arc cross-sections into annuli in each of which the plasma properties $\sigma$, $K$ and $P$ were assumed to be constant, as illustrated in Fig. 1. Clearly, the smaller the width of the annular zone, the smaller are the changes in $\sigma$, $K$ and $P$ between zones. In the limit, $\sigma$, $K$ and $P$ vary continuously with radius.

All the calculations reported above were made using an annular width of 0·01 cm or less, depending on the electric field. This meant in practice that in all cases the arc cross-section was divided up into never less than 75 zones. In a separate calculation corresponding to the conditions $T_o = 15\,500$°K, E = 10 volts/cm the temperature distribution, arc radius, current and radiation were calculated using an annular width of 0·002 cm as well as the usual width of 0·01 cm. The results are summarised in Table 3.

In addition the two temperature distributions never varied by more than 3 per cent over the whole temperature range down to 5000°K; over the temperature range from 15 500°K to 10 000°K, the variation was much less than 1 per cent.

The above results show that use of the larger annular widths do not introduce substantial losses in accuracy in view of the other potential sources of error mentioned above.

5. *Conclusions.*

Numerical solutions of the energy balance equation for an axially-symmetrical uniform arc column have been described and illustrated with some results obtained for a nitrogen plasma at atmospheric pressure. Calculations of temperature distribution, arc currents, arc radii and radiation loss were used to illustrate anomalies which exist between various sets of published data for the electrical conductivity, $\sigma$, the thermal conductivity $K$ and the radiated power density $P$, of nitrogen at atmospheric pressure. The

temperature distributions, arc current, arc radii and radiation losses computed in this way were compared with published information of experimental measurements of these same properties. These comparisons provide a rational basis for the rejection of those sets of plasma property data which gave results inconsistent with the experimental measurements. What are regarded as the best available data on the variation of electrical conductivity, thermal conductivity and radiated power density of nitrogen at 1 atmosphere with temperature were then selected for use in further calculations of arc properties. These data are summarised by Figs. 2, 3 and 4 and also by Table 1.

The effects of radiation cooling on arc columns of different sizes were then examined. It was found that radiation losses could be minimised by operating arc columns in narrow channels even though large electric fields, $E$, were required to sustain the current. When $P/\sigma E^2$ was much less than unity, it was found that the simpler, radiation neglected, arc column theory as discussed by King[14] could be used.

Lord's[15] dimensional analysis of arc columns was then outlined and his proposed similarity parameters $EI$–$U$, $I/ER^2$, $U/R^2$ were tested using computed arc properties, $I$, $U$ and $R$ for a range of values of $E$, axial temperature $T_o$, and arc boundary temperature $T_R$.

The proposed laws of similarity were found to be satisfied to within the accuracy of the computations. Following this, the dependence of the above similarity groups on $T_o$ and $T_R$ was investigated. The results are shown in a set of universal curves—Figs. 8 to 10.

Using the universal curves, one can determine arc properties such as the radiation loss or the axial temperature $T_o$ from measurements of arc radius $R$, arc current $I$ and voltage gradient $E$. These curves were prepared in conjuction with an investigation into arcs driven by magnetic fields.

*Acknowledgments.*

I wish to thank Mr. L. A. King of the English Electric Company, and previously of the Electrical Research Association, Leatherhead, for making available to me the results of his unpublished calculations of the electrical and thermal conductivities of nitrogen plasmas. I also wish to thank Dr. H. Pelzer, also of the Electrical Research Association, Leatherhead, for his valuable comments and advice concerning re-calculation of the radiation data.

---

## LIST OF SYMBOLS

| | |
|---|---|
| $c$ | Velocity of light |
| $e$ | Electronic charge |
| $g$ | Statistical weight of an electronic energy state |
| $h$ | Planck's constant |
| $k$ | Boltzmann's constant |
| $l$ | Quantum number |
| $m$ | Electronic mass |
| $n$ | Quantum number |
| $q$ | Heat flux |
| $r$ | Radial co-ordinate |

| | |
|---|---|
| $v_j$ | Thermal velocity of $j^{th}$ species (electron, atom, ion, etc.) |
| $C_{vj}$ | Specific heat per particle of $j^{th}$ species |
| $E$ | Voltage gradient |
| $E_H$ | Ionization energy of the hydrogen atom |
| $E_i$ | Ionization energy |
| $E_{nl}$ | Excitation energy of electronic state with quantum numbers $n$, $l$ |
| $G_F(v, T)$ | Gaunt factor for free electrons as a function of frequency and temperature |
| $G_{nl}(v)$ | Gaunt factor for bound electronic states with quantum numbers $n$, $l$ |
| $I$ | Current |
| $J$ | Total radiation flux |
| $K(T)$ | Thermal conductivity |
| $N_e$ | Electron number density |
| $N_i$ | Ion number density |
| $N_j$ | Number density of $j^{th}$ species |
| $N_o$ | Neutral number density |
| $P(T)$ | Radiated power density |
| $Q$ | Heat conducted through unit length of arc boundary |
| $Q_{ie}$ | Ion-electron collision cross-section |
| $Q_{oe}$ | Neutral-electron collision cross-section |
| $R$ | Arc radius |
| $T$ | Temperature |
| $U$ | Radiation loss from unit length of arc column |
| $W$ | Power input to unit length of arc column |
| $Z$ | Ionic charge |
| $\lambda_c$ | Classical electron mean free path |

| | |
|---|---|
| $\lambda_j$ | Mean free path of $j^{th}$ species in collisions with all other particles |
| $\mu_e$ | Electron mobility |
| $\sigma(T)$ | Electrical conductivity |
| $\nu$ | Frequency |

*Suffixes*

| | |
|---|---|
| $i$ | Referring to $i^{th}$ annulus |
| $o$ | Referring to axis of arc column |
| $R$ | Referring to arc periphery |

---

## REFERENCES


| *No.* | *Author(s)* | *Title, etc.* |
|---|---|---|
| 1 & 2 | V. W. Adams .. .. | The influence of gas streams and magnetic fields on electric discharges.<br>Part 1—Arcs at atmospheric pressure in annular gaps.<br>Part 2—The shape of an arc rotating an annular gap.<br>A.R.C. C.P. 743 (1963) |
| 3 | V. W. Adams .. .. | The influence of gas streams and magnetic fields on electric discharges.<br>Part 3—Arcs in transverse magnetic fields at atmospheric pressure. |
| 4 | W. T. Lord .. ..<br>E. G. Broadbent .. .. | An electric arc across an air stream.<br>R.A.E. Technical Report 65055 (A.R.C. 26,847) (1965). |
| 5 | W. T. Lord .. .. | Effect of a radiative heat sink on arc voltage-current characteristics.<br>Proceedings of a Specialists Meeting on Arc Heaters and M.H.D. Accelerators for Aerodynamic Purposes.<br>AGARD Fluid Dynamics Institute, Belgium, (1964).<br>AGARDograph *84*, Part 2, 673 (A.R.C. 26,695). |
| 6 | G. L. Marlotte .. ..<br>R. L. Harder<br>R. W. Prichard | AGARDograph *84*, Part 2, 633 (1964). |
| 7 | L. A. King .. .. | Unpublished results. |
| 8 | J. Yos .. .. .. | Theoretical and experimental investigation of arc plasma—Generation Technology.<br>Part II, Vol. 2, AVCO RAD–TR–63–12, ASD–TDR–62–729 (1964). |
| 9 | J. Uhlenbusch .. .. | Berechnung der Materialfunctionen eines Stickstoff—und Argon plasmas aus gemessen–Bogendaten.<br>*Zeit. f. Physik, 179*, 347, (1964). |

REFERENCES—*continued*


| | | |
|---|---|---|
| 10 | A. Monterde-Garcia . . | Materialfunctionen von Bogenplasmen aus Charakteristikmessungen.<br>*Zeit. f. Physik, 181*, 317 (1964). |
| 11 | F. Burhorn . . . . | Plasma densities of nitrogen pressure at 1, 3, 10 and 30 amps at temperatures between 1000°K and 30 000°K.<br>*Zeit. Phys. Chemie* (Liepzig)<br>*213*, 37, (1960).<br>*215*, 269, (1960).<br>*215*, 285, (1960). |
| 12 | H. Pelzer . . . . . | Electrical Research Association Unpublished Technical Report. |
| 13 | H. Maecker . . . . | The properties of nitrogen up to 15 000°K.<br>AGARD Report 324 (1959).<br>*Proc. 4th Int. Conf. Ion. Phen in Gases.*<br>Uppsala (1959).<br>Vol. I, p. 378, Amsterdam: North Holland Publ. Co. |
| 14 | L. A. King . . . . | Theoretical calculations of arc temperatures in different gases.<br>*Colloquium Spectroscopicum Internationale VI*, Amsterdam, p. 152.<br>Pergammon Press, London (1956). |
| 15 | W. T. Lord . . . . | Unpublished work. |
| 16 | A. Wells . . . . . | The influence of gas streams and magnetic fields on electric discharges—Part 7.<br>Unpublished Ministry Report. |
| 17 | J. D. Craggs . . . .<br>H. Edels | Thermal and electrical conductivities of plasmas.<br>*Progress in Dielectrics 5*, 187, Heywood and Co. Ltd. (1963). |
| 18 | J. O. Hirschfelder . .<br>C. F. Curtis<br>R. B. Bird | *Molecular theory of gases and liquids.*<br>Wiley, New York (1954) |
| 19 | S. Chapman . . . .<br>T. G. Cowling | *The mathematical theory of non-uniform gases.*<br>2nd. Edition. Cambridge University Press (1952). |
| 20 | E. A. Guggenheim . . | *Elements of the kinetic theory of gases.*<br>Pergammon Press (1960). |
| 21 | H. Pelzer . . . . . | On the contributions of dissociation and ionization to the thermal conductivity of gas.<br>*Proc. Vth Int. Conf. Ion. Phen. in Gases.*<br>North Holland Publ. Co. Vol. 1, 846, Munich (1961). |
| 22 | F. Burhorn . . . . | Berechnung Messung der Wärmeleitfähigkeit von Stickstoff bis 13 000°K.<br>*Zeit. f. Physik 155*, 42, (1959). |
| 23 | H. R. Griem . . . . | Plasma spectroscopy.<br>McGraw Hill (1964). |
| 24 | A. Unsöld . . . . . | Physik der Sternatmosphären.<br>2nd Edition, Springer, Berlin 163–74 (1955) |

25 G. Buss .. .. .. Thermische Lichtbögen hoher Temperatur und niedriger Brennspannung.
W. Finkelnberg .. .. *Zeit. f. Physik 139*, 212 (1954)

26 E. G. Broadbent .. .. A theoretical exploration of the flow about an electric arc transverse to an airstream using potential flow methods.
A.R.C. R. & M. 3531 (1965).

---

## APPENDIX A

*Theoretically Derived Transport and Radiative Properties of Arc Plasmas*

In this Appendix, the formulae generally used to calculate the coefficients of the electrical conductivity, $\sigma$, and thermal conductivity, $K$, of an equilibrium arc plasma are summarised. Results obtained by different authors are compared.

Theory relating to the total radiation loss from arc plasmas is also reviewed and calculations by the author of radiated power density from nitrogen at atmospheric pressure are compared with the results of other workers.

*A.1. Electrical Conductivity of Nitrogen at 1 Atmosphere.*

Electrons and ions are present in equal concentrations in an arc plasma in thermal equilibrium. However, the electric current in an arc plasma is carried principally by electrons by virtue of the fact that electrons are of the order $10^4$ times lighter than nitrogen ions and are therefore much more readily accelerated by the electric field. The electrical conductivity depends both on the electron concentration, $N_e$, and on the electron mobility, $\mu_e$, in the electric field. Both these quantities are temperature dependent.

$$\sigma = N_e e \mu_e . \tag{A.1}$$

The electron concentration in an equilibrium plasma at constant pressure is generally determined theoretically by solving the Saha equation for each plasma constituent assuming the arc plasma to be electrically neutral, to be in thermal equilibrium and to obey the ideal gas law. There have been many calculations of the concentrations of plasma constituents based on the Saha equation. An example of the results of Burhorn and Wienecke[11] for a nitrogen plasma in the temperature range 5000°K to 35 000°K at one atmosphere is given in Fig. 11.

The electron mobility is generally calculated using Langevin's mobility equations (*see* Edels and Craggs[17] for example).

$$\mu_e = \frac{e \lambda_c}{(3mkT)^{\frac{1}{2}}} . \tag{A.2}$$

In equation (A.2), $\lambda_c$, is the classical electron mean free path for electron-atom and electron-ion collisions. These collisions result in randomisation of the directed velocity acquired by electrons that have been accelerated by the electric field. $\lambda_c$ depends on the cross-section for electron-atom or electron-ion collisions.

According to simple kinetic theory, the electron mean free paths depend on a classical collision cross-section $Q$, according to equation (A.3)

$$\lambda_c = \frac{1}{N_o Q_{oe} + N_i Q_{ie} + \ldots}. \tag{A.3}$$

More sophisticated calculations of mean free paths make use of the concept of the collision integral introduced by Hirschfelder, Curtis and Bird[18].

The values of collision cross-sections used by various authors in their calculations of $\sigma$ vary over quite wide ranges thus accounting for most of the discrepancies which exist between published data.

The results of theoretical calculations by King[7,14], and Yos[8], of the electrical conductivity of nitrogen at 1 atmosphere are compared in Fig. 2.

A.2. *Thermal Conductivity of Nitrogen at 1 Atmosphere.*

In their review article on the 'Thermal and Electrical Conductivities of High Temperature Gases', Edels and Craggs[17] discuss the contributions to the total thermal conductivity due to:

(a) a heat flux, $q_c$, in which translational and internal energy of the plasma constituents are transported down a temperature gradient,

(b) a heat flux, $q_d$, associated with the interdiffusion of reacting species,

(c) a heat flux, $q_t$, associated with the diffusion thermo-effect.

Thermal conductivity is then given by:

$$(q_c + q_d + q_t) = -K\nabla T = -(K_c + K_d + K_t)\nabla T. \tag{A.4}$$

The results of the kinetic theory of non-uniform gases (Chapman and Cowling[19]; Hirschfelder, Curtis and Bird[18]) are very complicated particularly for multi-constituent plasmas, and most workers use approximate formulae derived from elementary kinetic theory (e.g. Guggenheim[20]) in order to calculate thermal conductivities.

The component, $K_c$, of the thermal conductivity due to the transport of translation, vibration, rotation and excitation energy of the plasma particles is, according to elementary kinetic theory:

$$K_c = \frac{1}{3}\Sigma N_j \bar{v}_j \lambda_j Cv_j \tag{A.5}$$

summed for all constituents in the plasma.

$N_j$ is the concentration of the $j^{\text{th}}$ constituent (i.e. molecules, atoms, ions or electrons)

$\bar{v}_j$ is the mean thermal velocity of the constituent

$Cv_j$ is the specific heat per particle at constant volume

$\lambda_j$ is the mean free path for particles of the $j^{\text{th}}$ type incollisions with all other particles.

Approximate expressions for the component, $K_d$, of the thermal conductivity due to the interdiffusion of reacting species are given by Edels and Craggs[17], Yos[8], Pelzer[21], and Burhorn[22]. In nitrogen at temperatures at which the plasma is either partly dissociated or partly ionized, the contribution to the total thermal conductivity from $K_d$, is quite large. In the case of dissociation, gradients in atomic and molecular concentrations are present whenever temperature gradients exist in the arc plasma, as Fig. 11 indicates. In this situation atoms diffuse away from the regions of higher temperature and higher atom concentration and recombine at lower temperatures when super-elastic collisions with other particles become sufficiently frequent. As a result of these collisions the recombination energy of pairs of recombining atoms is transferred to the colliding particles as kinetic energy. The excess concentration of molecules

at the lower temperatures correspondingly leads to a diffusion flux of molecules against the temperature gradient and the diffusing molecules dissociate at the higher temperature having first absorbed the necessary dissociation energy in collisions with other particles. Some dissociation energy is, in effect, transported down the temperature gradient by this diffusion process, the total thermal conductivity of the plasma is thereby enhanced. The interdiffusion of atoms, ions and electrons in ionization zones in arc plasmas similarly leads to an enhancement of the thermal conductivity due to the transport of ionization energy down the temperature gradient.

The rate of transfer of reaction energy which determines $K_d$, depends on the diffusion coefficient for interdiffusion of species. In the case of the dissociation reaction the diffusion coefficient depends on the cross-sections for collisions of atoms with molecules and molecules with atoms. In the case of the ionization reaction, the atom-ion charge transfer collision cross-section determines the diffusion rate. There are very few published data on these types of collisions. Differences in the choice of numerical coefficients of these cross-sections by various workers accounts for most of the differences in the published data on thermal conductivities.

The diffusion thermo-effect is the transport of heat due to concentration gradients in a multicomponent gas mixture. The effect contributes very little to the total thermal conduction process in arc plasmas except in the case of electrons interdiffusing with ions. Edels and Craggs have derived an expression for $K_t$ for electrons.

Total thermal conductivities of nitrogen at 1 atmosphere have been calculated by King[7,14], Yos[8], Burhorn[22] and others. King's[7] and Yos's[8] results are compared in Fig. 3.

A.3. *Radiated Power Density of Nitrogen at 1 Atmosphere.*

A detailed treatment of the radiation from an equilibrium nitrogen plasma involves considering the processes of emission of radiation and also the processes of subsequent absorption of this radiation. In the theoretical treatments which lead to the results given in Fig. 4, not only are absorption effects neglected (the optically thin approximation) but also the physical processes of emission are grossly over-simplified so as to permit theoretical expressions for spectral radiated power density to be integrated over the whole frequency spectrum. It is as a result of different simplifications used by different authors that the theoretical results differ from one another.

Radiation from arc plasmas arises from:

(i) the line spectra of atoms and atomic ions;

(ii) the band spectra of molecules and molecular ions;

(iii) the continuum spectra of radiative free-free and free-bound (recombination) electron-ion interactions.

It turns out that energy radiated in line and band spectra is negligible compared with the continuum radiation in arc plasmas. Griem[23] has, recently, given a very full account of the factors which contribute to the continuum radiation emitted by a plasma. The earlier numerical calculations of Pelzer[12] and of Yos[8] include a number of approximations to Griem's results and it is in the nature of these approximations that reasons for differences between the results of these two authors are to be found. In relatively simplified terms, the spectral emission coefficient at frequency $\nu$ is given by Griem as:

$$\varepsilon_\nu = \frac{128\,\pi^4\, m\, Z^4\, e^{10}}{3^{3/2}\,(2\pi m\, kT)^{3/2}\, h^2\, c^3}\, N_e\, N_i \exp\left(-\frac{\Delta E_i - h\nu}{kT}\right)\left[\frac{\Sigma'\, G'_{nl}(\nu)\, g^o_{nl}}{n^3\, g^i_o}\exp\left(\frac{E_i - E_{nl}}{kT}\right)+\right.$$

$$\left.+\frac{\Sigma''\, G''_n(\nu)}{n^3}\exp\left(\frac{Z^2\, E_H}{n^2\, kT}\right)+\frac{G_F(\nu, T)\, kTh^2}{2Z^2\,(2\pi^2\, e^4\, m)}\exp\left(\frac{Z^2\, E_H}{n_1^2\, kT}\right)\right]. \qquad \text{(A.6)}$$

In the common factor preceding the square brackets in this expression:

$N_e$ and $N_i$ refer to the electron and ion densities respectively,

$\Delta E_i$ is the depression of the ionization potential of gas atoms in the plasma microfield,

$\nu$ is the frequency of the emitted radiation,

$Z$ is the ionic charge;

all other symbols have their usual meaning.

The first term inside the square brackets refers to the radiation emitted as a result of all electron-ground state ion recombination into a low-lying bound atomic state, such that wavefunctions of electrons in these states differ appreciably from the electronic wavefunctions in a hydrogen atom in the corresponding quantum state. In this term $E_{nl}$ is the energy of such a state with quantum numbers $n$, $l$ and statistical weight $g^o_{nl}$,

$E_i$ is the ionization energy of the atom,

$g^i_o$ is the statistical weight of ground state ions.

$G'_{nl}(\nu)$, the Gaunt factor corresponding to these radiative transitions has been calculated by Anderson and Greim for hydrogen, helium, carbon, nitrogen and oxygen (Griem[23], Table 5.8).

The second term inside the square brackets refers to radiative recombinations at higher states of quantum number $n$ for which the hydrogenic approximation is reasonably valid. In this term $G''_n(\nu)$ is the hydrogenic Gaunt factor also given by Griem. The energy of these quasi-hydrogenic states are such that

$$\frac{Z^2 E_H}{n^2} = E_i - E_n \tag{A.7}$$

where $E_H$ is the ionization energy of hydrogen $= 13{\cdot}59\, eV$.

The third term refers to free-free radiative transitions and includes recombination into atomic states which are merged with adjacent states such as occurs near series limits. In this term $G_F(\nu, T)$ is the free-free Gaunt factor given by Griem[23];

$n_1$, is the quantum number of the lowest merged state in the atom and is such that

$$\frac{Z^2 E_H}{n_1^2} = \begin{matrix} \Delta E_s \\ \text{or } h\nu + \Delta E_i \text{ whichever is the smaller} \end{matrix} \tag{A.8}$$

and $\Delta E_s$ is the depression of the series limit due to merging of high quantum number energy levels.

Equation (A.6) refers specifically to the formation of neutral atoms by radiative recombination (putting $Z = 1$) but it can also be used to deal with radiation due to recombination of electrons with doubly or more high ionized ions. However, recombination between electrons and excited ions is not covered by the equation.

The data of Yos and of Pelzer calculated using a number of approximations to Griem's expression.

Yos ignored all recombination into bound states and assumed the continua of states extended over the whole range of photon energies radiated in the recombination spectrum, that is

$$\frac{Z^2 E_H}{n_1^2} = h\nu + \Delta E_i \text{ in equation (A.8)}.$$

Also, assuming $G_F(\nu, T) = 3$, he obtained the total radiation emitted per unit volume of plasma at temperature $T$:

$$P = \int_\nu 4\pi \varepsilon_\nu \, d\nu = \frac{128\pi^3 e^6 N_e \Sigma N_i Z^2}{3^{\frac{1}{2}} (2\pi m)^{3/2} c^3 (kT)^{\frac{1}{2}}} \int_\nu d\nu \tag{A.9}$$

where the integration takes place over a frequency range $\Delta\nu$ which Yos assumed to be given by:

$$\Delta\nu = \frac{4kT}{h}. \tag{A.10}$$

Errors are introduced into Yos's calculations by virtue of:

(i) the assumed Gaunt factor which appears excessively large;

(ii) the choice of an arbitrary frequency waveband, and

(iii) the recombination into lower bound states which he ignores.

Pelzer[12] has avoided the problem relating to the frequency limits of the integration. Following Unsold's[24] treatment of total continuum radiation from stellar plasmas, Pelzer assumed that all states above a certain energy level, $E_{n_1}$, ($3S^4P$ level in atomic nitrogen) are sufficiently closely spaced to be regarded as an energy continuum. That is:

$$\frac{Z^2 E_H}{n_1^2} = E_i - E_{n_1} = h\nu_g \text{ in equation (A.8)}$$

for low frequencies such that $h\nu \leqslant E_i - E_{n_1}$, equation (A.6) combined with (A.8) gives an emission coefficient:

$$\varepsilon_\nu \, d\nu = \frac{G_F \cdot 32\pi^2 e^6 N_e \Sigma Z^2 N_i}{3^{3/2} (2\pi m)^{3/2} (kT)^{\frac{1}{2}} c^3} d\nu \tag{A.11}$$

which is essentially the same as used by Yos. However, for frequencies such that $h\nu > E_i - E_{n_1}$, equations (A.6) combined with (A.8)

$$\varepsilon_\nu \, d\nu = \frac{G_F \cdot 32\pi^2 e^6 N_e \Sigma Z^2 N_i}{3^{3/2} (2\pi m)^{3/2} (kT)^{\frac{1}{2}} c^3} \exp -\left(\frac{\Delta E_i + h(\nu - \nu_g)}{kT}\right) d\nu. \tag{A.12}$$

Thus Pelzer obtained the total radiated power from unit volume of plasma at a temperature $T$ by integration of equation (A.11) over the frequency range from 0 to $\nu_g$ and equation (A.12) containing the additional exponential factor over the frequency range $\nu_g$ to infinity and then multiplying by $4\pi$. He obtained the result:

$$P = \frac{G_F \cdot 128\pi^3 e^6 N_e \Sigma Z^2 N_i}{3^{3/2} c^3 (2\pi m)^{3/2} h} (kT)^{\frac{1}{2}} \left(\frac{h\nu_g}{kT} + 1\right). \tag{A.13}$$

Pelzer also estimated the magnitude of the radiation due to recombination into the bound $2p^3\ {}^4S$ (ground) state and the $2p^3\ {}^3D$ and $2p^3\ {}^2P$ low lying excited states in atomic nitrogen on the assumption that these states were essentially hydrogenic by nature. This corresponds to using the second term in equation (A.7). However, as Pelzer pointed out this radiation occurs in the vacuum ultra-violet, 850 Å to 1130 Å, and is unlikely to escape unabsorbed from an arc plasma, at atmospheric pressure.

Pelzer's original radiation calculations were made using a value of $Z = 1{\cdot}4$, $G_F = 1$ and $h\nu_g/k = 48\,000°K$ for singly ionized nitrogen. The author has recalculated Pelzer's radiation data making several modifications.

(i) On Pelzer's suggestion values $Z = 1{\cdot}1$ for singly ionized nitrogen and $Z = 2{\cdot}1$ for doubly ionized nitrogen were used.

(ii) The dependence of electron and ion density with temperature used by Pelzer was taken from data

given by Busz and Finkelnburg[25] which has subsequently been shown to be inaccurate. The more recent data of Burhorn and Wienecke[11] were used in the revised radiation calculations.

(iii) A revised value of $h\nu_g/k$ of 136 000°K was used for doubly ionized nitrogen, $\nu_g$ corresponding to the $2p^3\ {}^1D$ level in doubly ionized nitrogen.

With these modifications, the power radiated per unit volume was recalculated.

The data due to Yos, Pelzer (original) and Pelzer—modified (Wells) are shown in Fig. 4.

Using Griem's treatment it should now be possible to calculate plasma radiation densities which are much better founded on physical theory than the calculations discussed above. However, at the time that the arc energy balance calculations were initiated Griem's works had not been published. Also the revised calculations of radiated power density gave reasonably close agreement with experimentally derived values of the radiation density. Therefore, the incentive for embarking on long, laborious, theoretical derivations of radiated power density does not exist, because theoretically derived radiation data can now be replaced by experimental data which is equally concise.

---

## APPENDIX B

*Experimentally Derived Transport and Radiative Properties of Arc Plasmas*

In Appendix A, the theoretical derivations of the properties, electrical conductivity, $\sigma$, thermal conductivity, $K$, and radiated power density, $P$, of arc plasmas was outlined. Alternatively, these properties may be obtained directly or indirectly from experimental measurements on arc plasmas and these techniques have also received a great deal of attention in recent years.

Edels and Caggs[17] have reviewed measurements of electrical and thermal conductivities of arc plasmas made before 1963. Since then, however, a significant advance has been made through, on the one hand, the development of the wall stabilised arc column which is stable, reproducible, and uniform along its length (Maecker[13]) and, on the other hand, the development of techniques for analysing the voltage gradient current and radiation-current characteristics of these arc columns (Uhlenbusch[9], Monterde-Garcia[10]). The wall stabilised arc provide a means of measuring the voltage gradient-current ($E$–$I$) and radiation-current ($U$–$I$) characteristics of an arc with reasonable precision over wide ranges of current (from 0·1 to 300 amps). Also radial temperature distributions can be measured reasonably accurately in these columns.

Uhlenbusch and Monterde-Garcia have independently investigated methods of analysing experimental measurements on such wall stabilised arcs. In both cases they divide the arc cross-section up into a large number of annuli in each of which constant plasma properties ($\sigma$, $K$, $P$) are assumed. Using the energy balance equation,

$$\sigma E^2 - P + \frac{1}{r}\frac{d}{dr}\left(r\frac{d\phi}{dr}\right) = 0 \tag{B.1}$$

where

$$\phi = \int_0^T k\,dT \tag{B.2}$$

ohm's law

$$I = 2\pi E \int_0^R \sigma r \, dr \tag{B.3}$$

and the optically thin approximation of the radiation equation:

$$U = 2\pi \int_0^R P r \, dr \tag{B.4}$$

both authors perform a numerical inversion operation on the experimental $E$–$I$ and $U$–$I$ characteristics. From this they deduce the variation of $\sigma$ with $\phi$; $P$ with $\phi$; and the variation of $\phi$ with $r$ at various currents. Then using measured $T$–$r$ distributions, they are able to work out the variation of $\phi$ with $T$; from which the variation of $\sigma$ and $P$ with $T$ can be found. Finally, the thermal conductivity can be obtained by differentiating the $\phi$–$T$ curve.

Results of both Uhlenbusch's and Monterde-Garcia's analyses are shown on Figs. 2, 3 and 4 for comparison with the theoretical data discussed in Appendix A.

---

TABLE 1

*Electrical Conductivity, $\sigma$; Thermal Conductivity, K, and Radiated Power Density, P, of a Nitrogen Plasma at Atmospheric Pressure*

| T °K | $\sigma$ $(\Omega\text{–cm})^{-1}$ | K watts $cm^{-1}$ $°K^{-1}$ | P watts $cm^{-3}$ |
|---|---|---|---|
| 5000 | $4{\cdot}7 \times 10^{-3}$ | $7{\cdot}2 \times 10^{-3}$ | — |
| 6000 | $2{\cdot}3 \times 10^{-1}$ | $2{\cdot}79 \times 10^{-2}$ | — |
| 7000 | 2·0 | $3{\cdot}78 \times 10^{-2}$ | $2 \times 10^{-2}$ |
| 8000 | 12·0 | $1{\cdot}83 \times 10^{-2}$ | 1·1 |
| 9000 | 20 | $9{\cdot}95 \times 10^{-3}$ | 7·5 |
| 10 000 | 25·7 | $1{\cdot}22 \times 10^{-2}$ | $3{\cdot}9 \times 10^{1}$ |
| 11 000 | 35·0 | $2{\cdot}67 \times 10^{-2}$ | $1{\cdot}75 \times 10^{2}$ |
| 12 000 | 44·5 | $5{\cdot}06 \times 10^{-2}$ | $5{\cdot}38 \times 10^{2}$ |
| 13 000 | 51·5 | $1{\cdot}025 \times 10^{-1}$ | $1{\cdot}11 \times 10^{3}$ |
| 14 000 | 63·2 | $1{\cdot}48 \times 10^{-1}$ | $2{\cdot}14 \times 10^{3}$ |
| 15 000 | 73·7 | $1{\cdot}555 \times 10^{-1}$ | $3{\cdot}05 \times 10^{3}$ |
| 16 000 | 81·2 | $1{\cdot}471 \times 10^{-1}$ | $3{\cdot}28 \times 10^{3}$ |
| 17 000 | 88·1 | $1{\cdot}077 \times 10^{-1}$ | $3{\cdot}32 \times 10^{3}$ |
| 18 000 | 95·2 | $8{\cdot}30 \times 10^{-2}$ | $3{\cdot}13 \times 10^{3}$ |
| 19 000 | 100·7 | $7{\cdot}03 \times 10^{-2}$ | $2{\cdot}92 \times 10^{3}$ |
| 20 000 | 105·8 | $6{\cdot}50 \times 10^{-2}$ | $2{\cdot}67 \times 10^{3}$ |
| 21 000 | 109·9 | $6{\cdot}45 \times 10^{-2}$ | $2{\cdot}50 \times 10^{3}$ |
| 22 000 | 114·2 | $6{\cdot}67 \times 10^{-2}$ | $2{\cdot}35 \times 10^{3}$ |
| 23 000 | 116·9 | $6{\cdot}97 \times 10^{-2}$ | $2{\cdot}29 \times 10^{3}$ |
| 24 000 | 118·2 | $7{\cdot}28 \times 10^{-2}$ | $2{\cdot}42 \times 10^{3}$ |
| 25 000 | 117·8 | $7{\cdot}40 \times 10^{-2}$ | $2{\cdot}70 \times 10^{3}$ |
| 26 000 | 112·6 | $7{\cdot}38 \times 10^{-2}$ | $3{\cdot}07 \times 10^{3}$ |
| 27 000 | 106·5 | $7{\cdot}31 \times 10^{-2}$ | $3{\cdot}57 \times 10^{3}$ |
| 28 000 | 102·8 | $7{\cdot}21 \times 10^{-2}$ | $4{\cdot}18 \times 10^{3}$ |
| 29 000 | 99·2 | $7{\cdot}23 \times 10^{-2}$ | $4{\cdot}77 \times 10^{3}$ |
| 30 000 | 97·2 | $7{\cdot}27 \times 10^{-2}$ | $5{\cdot}11 \times 10^{3}$ |

TABLE 2

*Properties of a Nitrogen Arc at 1 Atmosphere.*

$T_0 = 15\,000°K$, $E = 25$ *V/cm.*

| Data | Yos[8] | King[14]/Pelzer[12] | Table 1 | Maecker experimental |
|---|---|---|---|---|
| Current (amps) | 54·8 | 241 | 219 | 200 |
| Radius at $T_R = 5000°K$ (cm) | 0·200 | 0·290 | 0·242 | 0·250 |
| Fraction of input Power lost as radiation | 0·077 | 0·095 | 0·047 | 0·048 |

TABLE 3

Calculated Properties of a Nitrogen Arc

$T_0 = 15\,500°K, E = 10\ V/cm$

| Annular zone width (cm) | Arc radius (cm) | Arc current (amps) | Radiation (k watts/cm) |
|---|---|---|---|
| 0·01 | 0·77 | 940·5 | 2·94 |
| 0·002 | 0·764 | 905·2 | 2·83 |

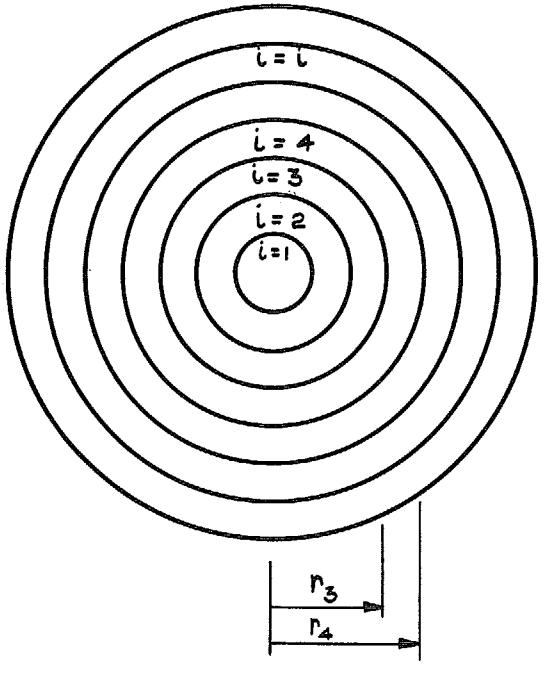


$i_{th}$ ANNULUS IS CONFINED WITHIN THE LIMITS $r_{(i-1)}$ TO $r_i$

PLASMA PROPERTIES $\sigma_i$, $K_i$ AND $P_i$ ARE ASSUMED CONSTANT THROUGHOUT THE $i_{th}$ ANNULUS.

VALUE OF $\sigma_i$, $K_i$ AND $P_i$ CORRESPOND TO TEMPERATURE $T_{(i-1)}$ (SEE TEXT)

FIG. 1. Theoretical model of cross-section of arc column.

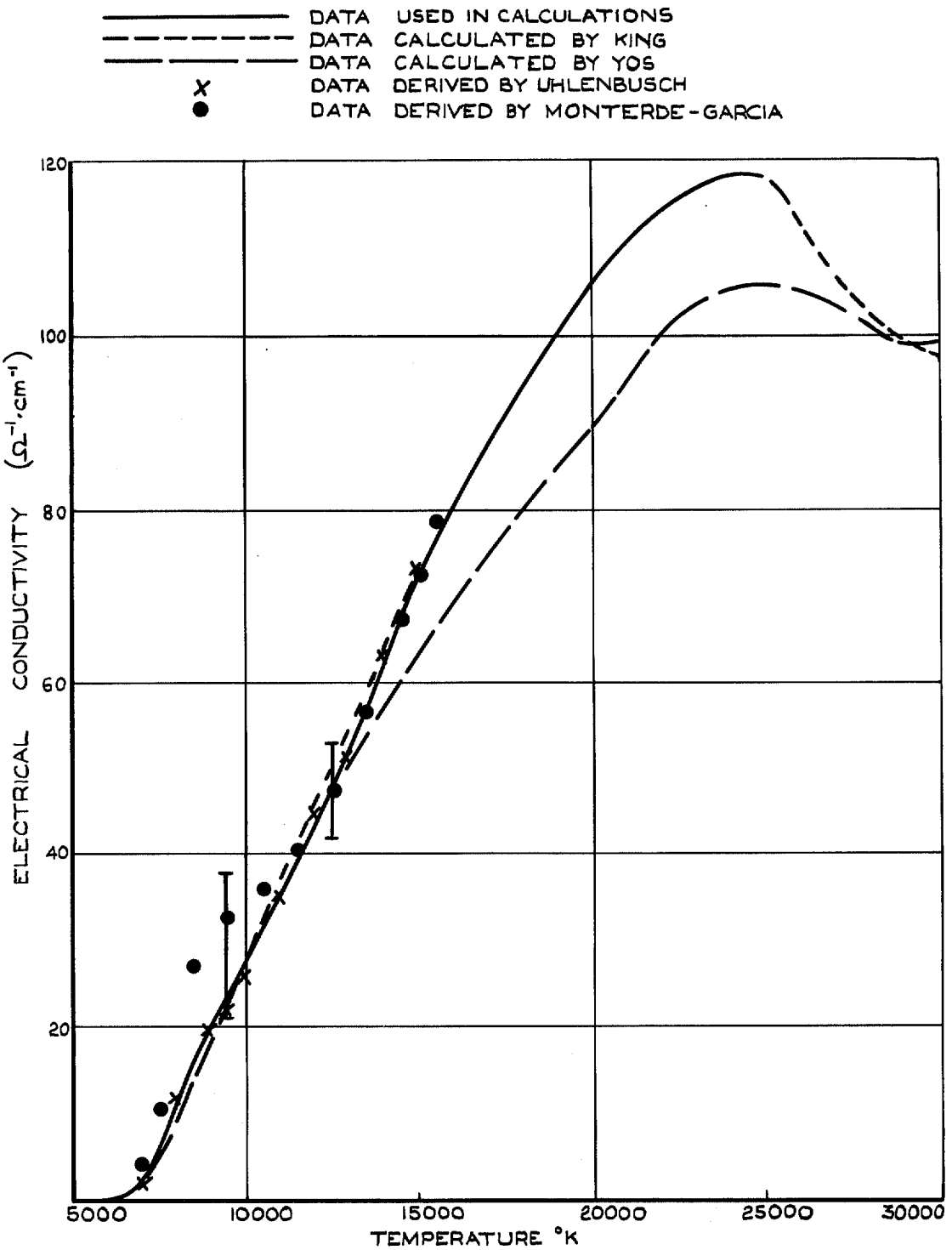


FIG. 2. Electrical conductivity of nitrogen plasma at atmospheric pressure.

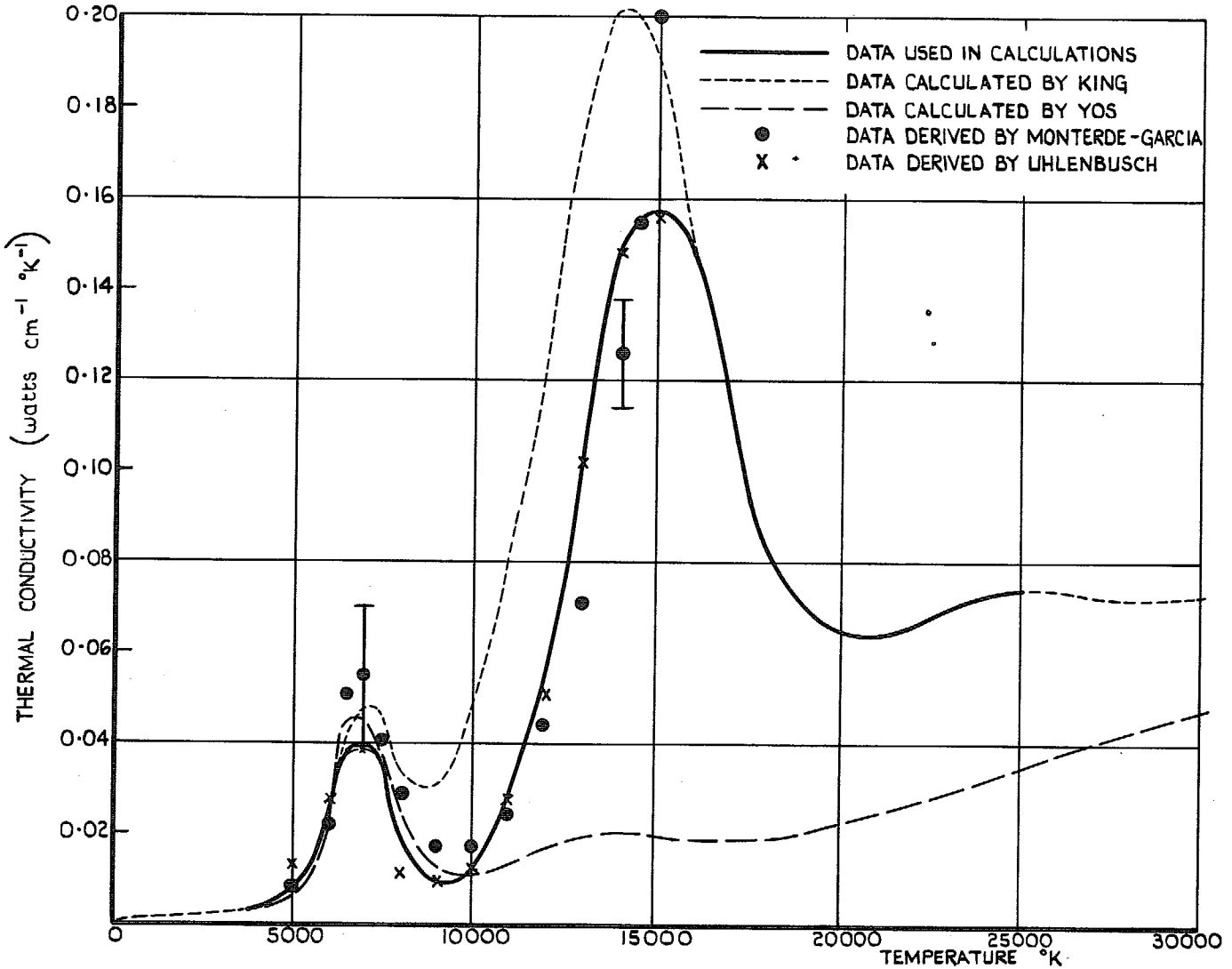


FIG. 3. Thermal conductivity of nitrogen plasma at atmospheric pressure.

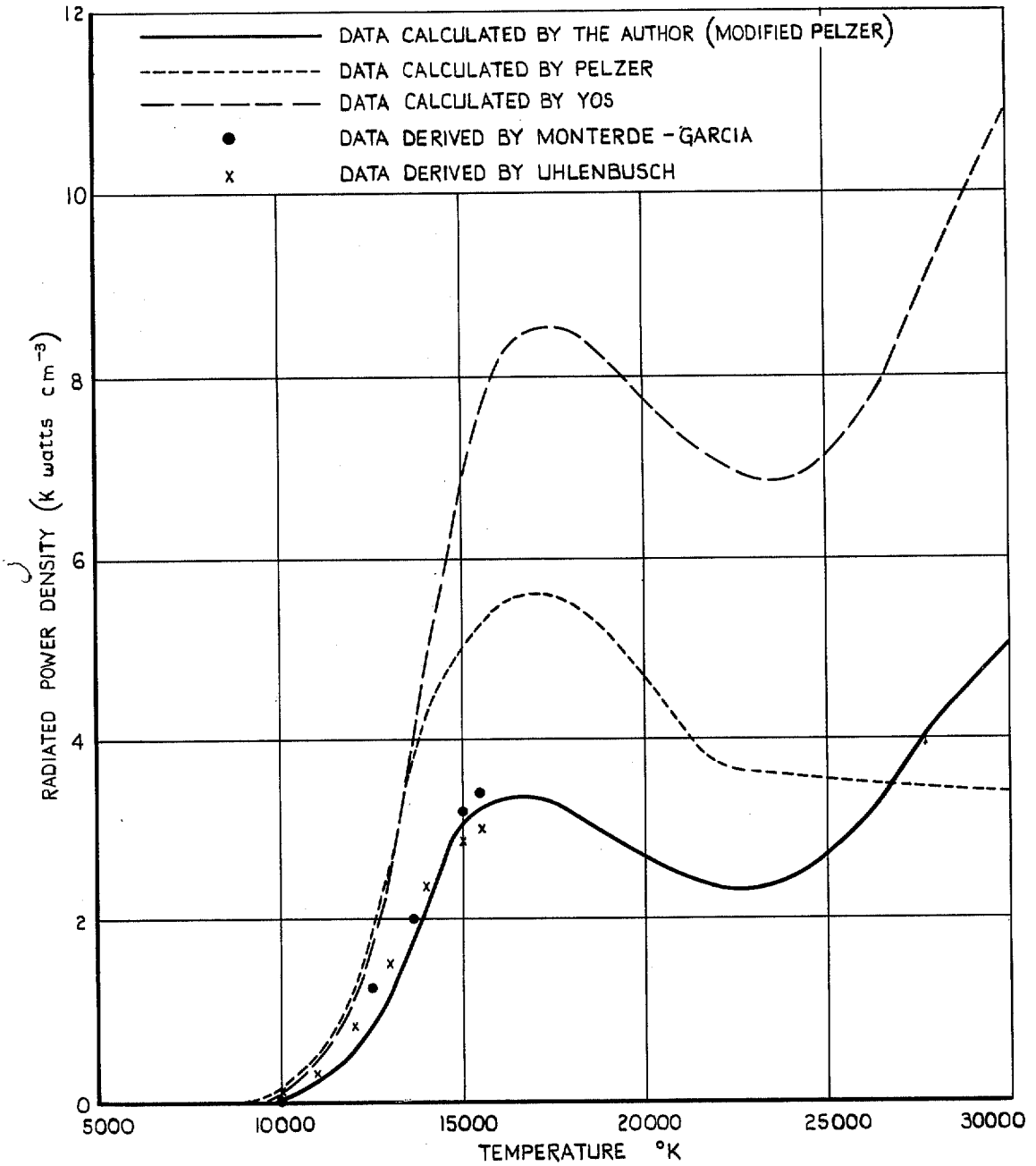


FIG. 4. Radiated power per $cm^3$ of nitrogen plasma at atmospheric pressure.

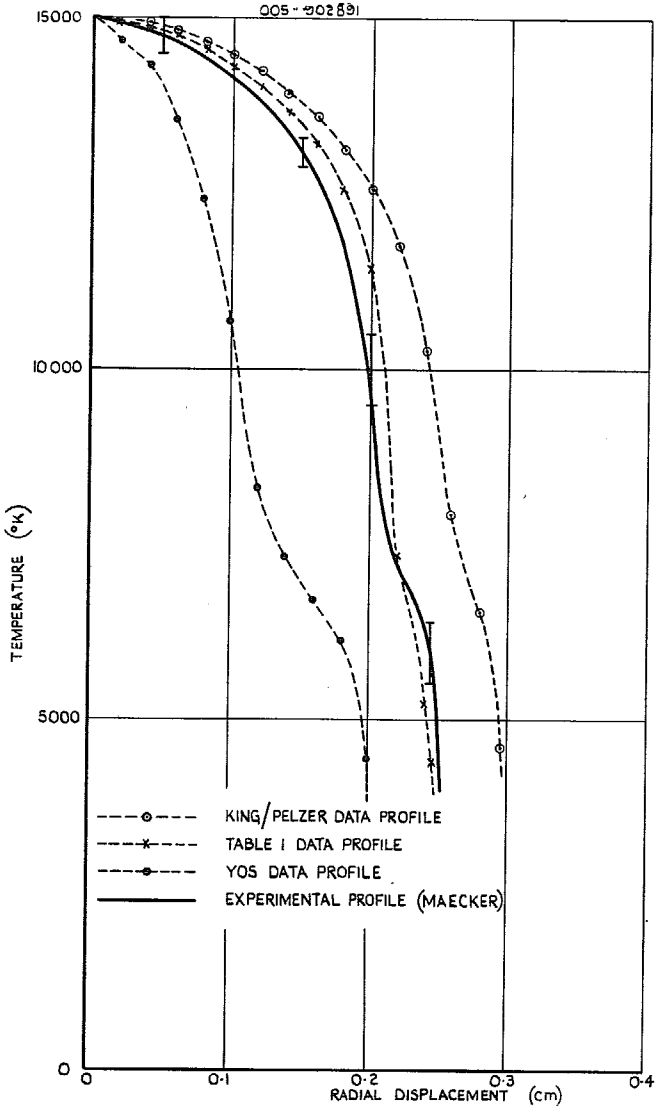


FIG. 5. Temperature distributions in a nitrogen arc at 1 atmosphere. $E = 25\ V/cm$ $T_0 = 15\,000°K$.

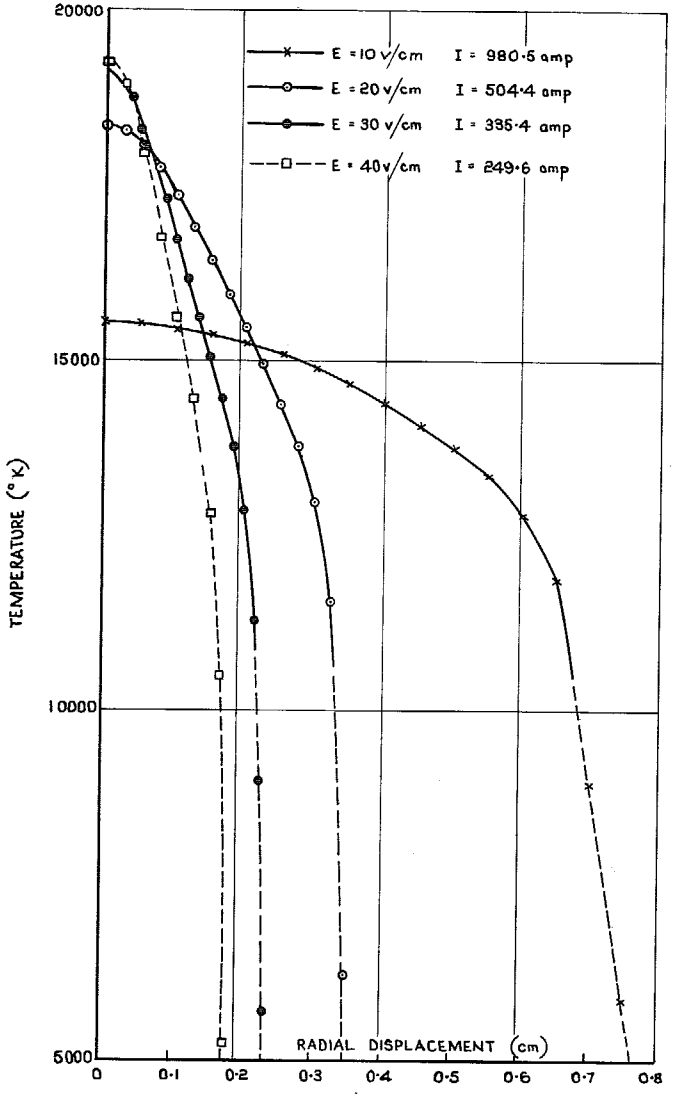


FIG. 6. Temperature distributions in a nitrogen arc at 1 atmosphere. Power unit 10 kwatts/cm of column.

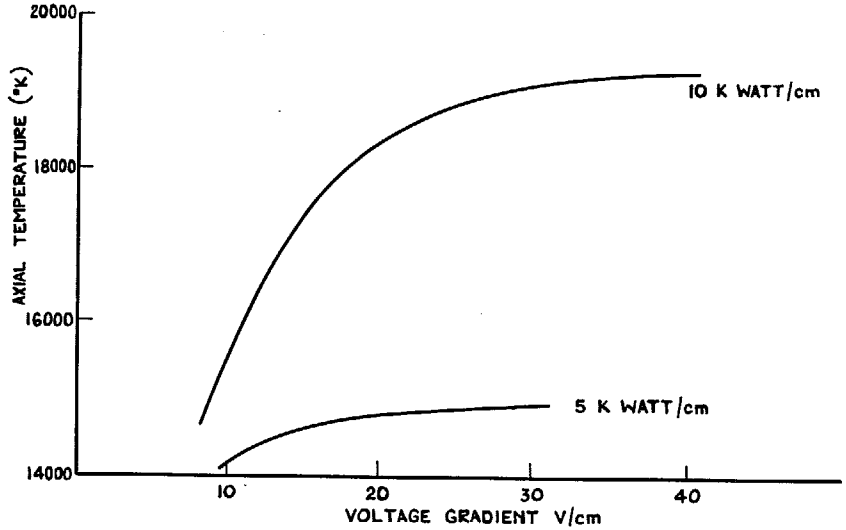


FIG. 7a. Variation of axial temperature with voltage gradient at constant power nitrogen arc at 1 atmosphere.

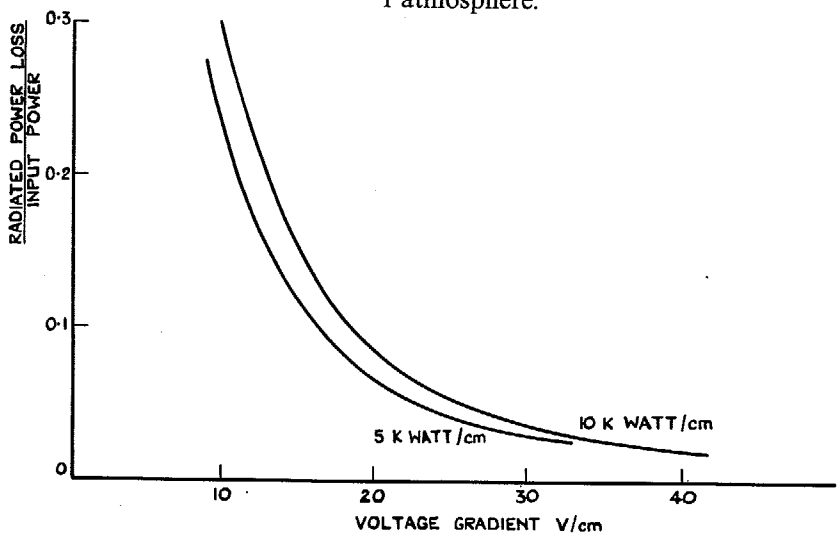


FIG. 7b Variation of radiation loss with voltage gradient at constant power nitrogen arc at 1 atmosphere

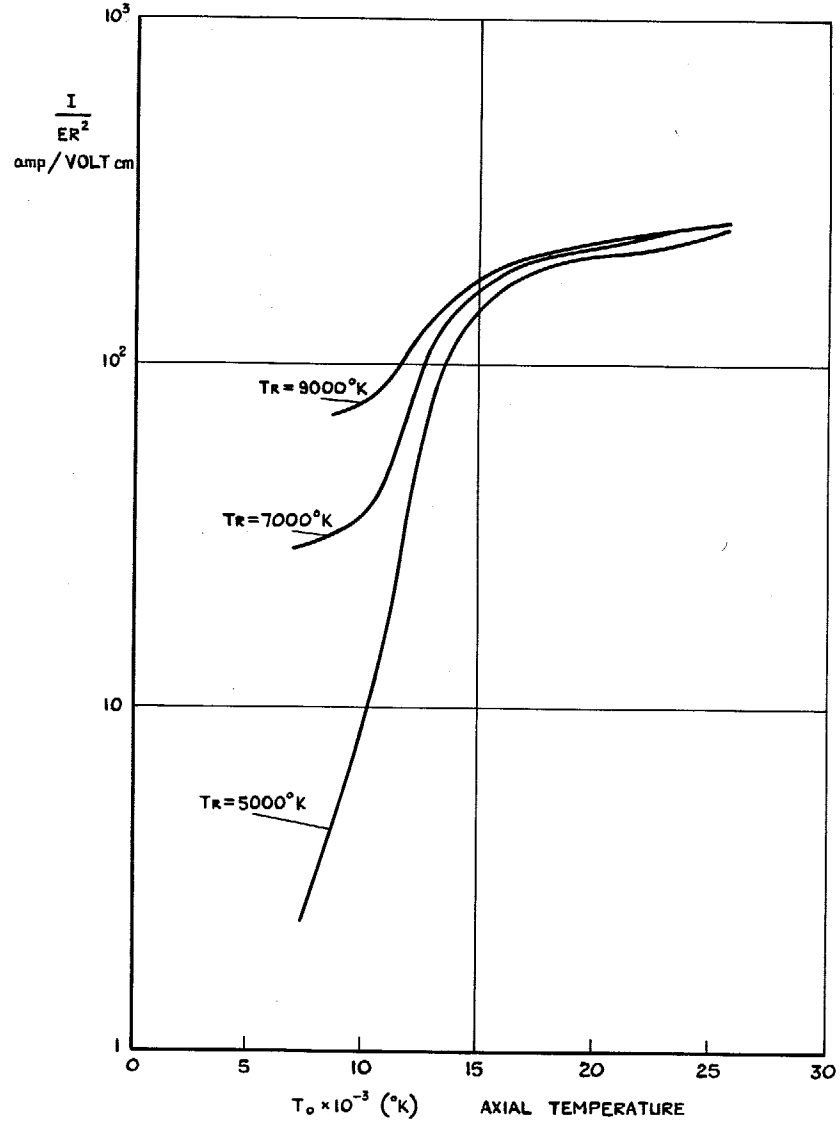


FIG. 8. Variation of current parameter $I/ER^2$ with axial temperature for arcs in nitrogen at atmospheric pressure.

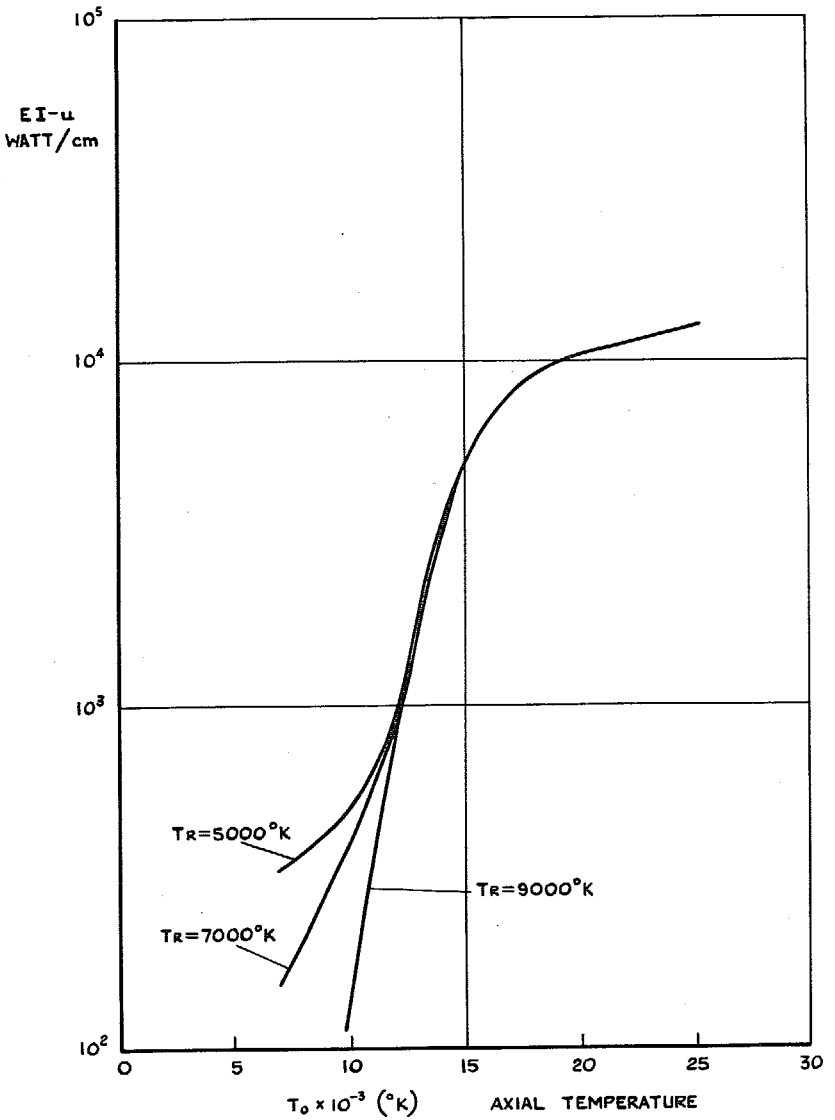


FIG. 9. Variation of conduction heat loss parameter *EI-u* with axial temperature for arcs in nitrogen at atmospheric pressure.

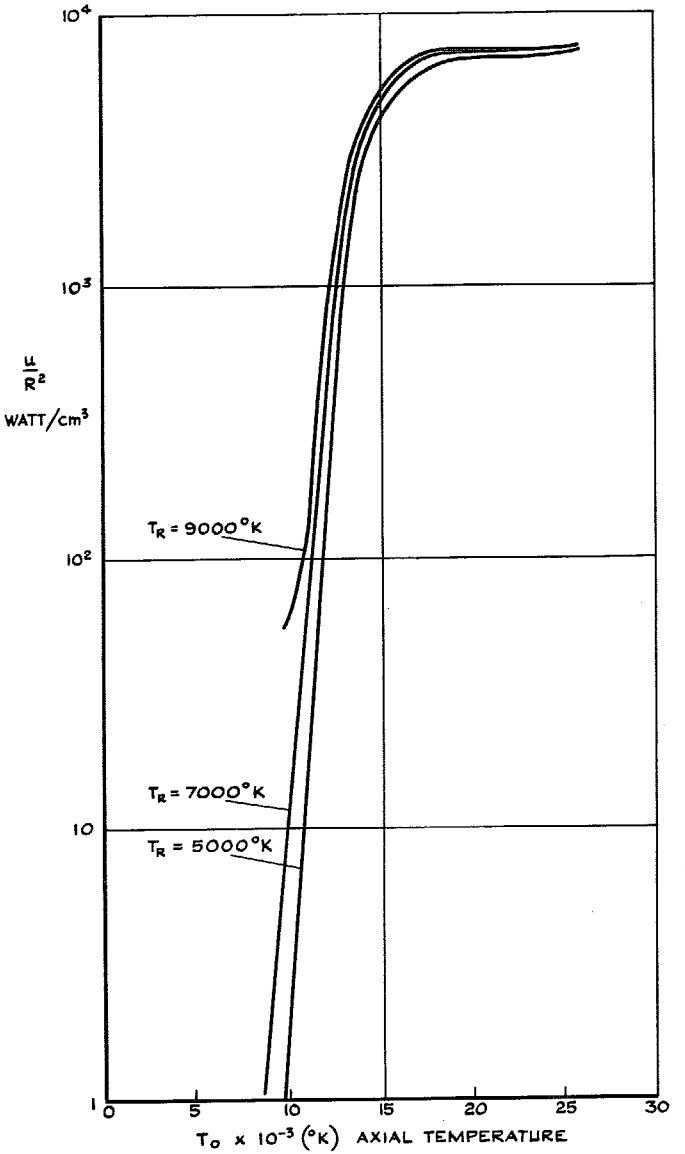


FIG. 10. Variation of radiation parameter $u/R^2$ with axial temperature for arcs in nitrogen at atmospheric pressure.

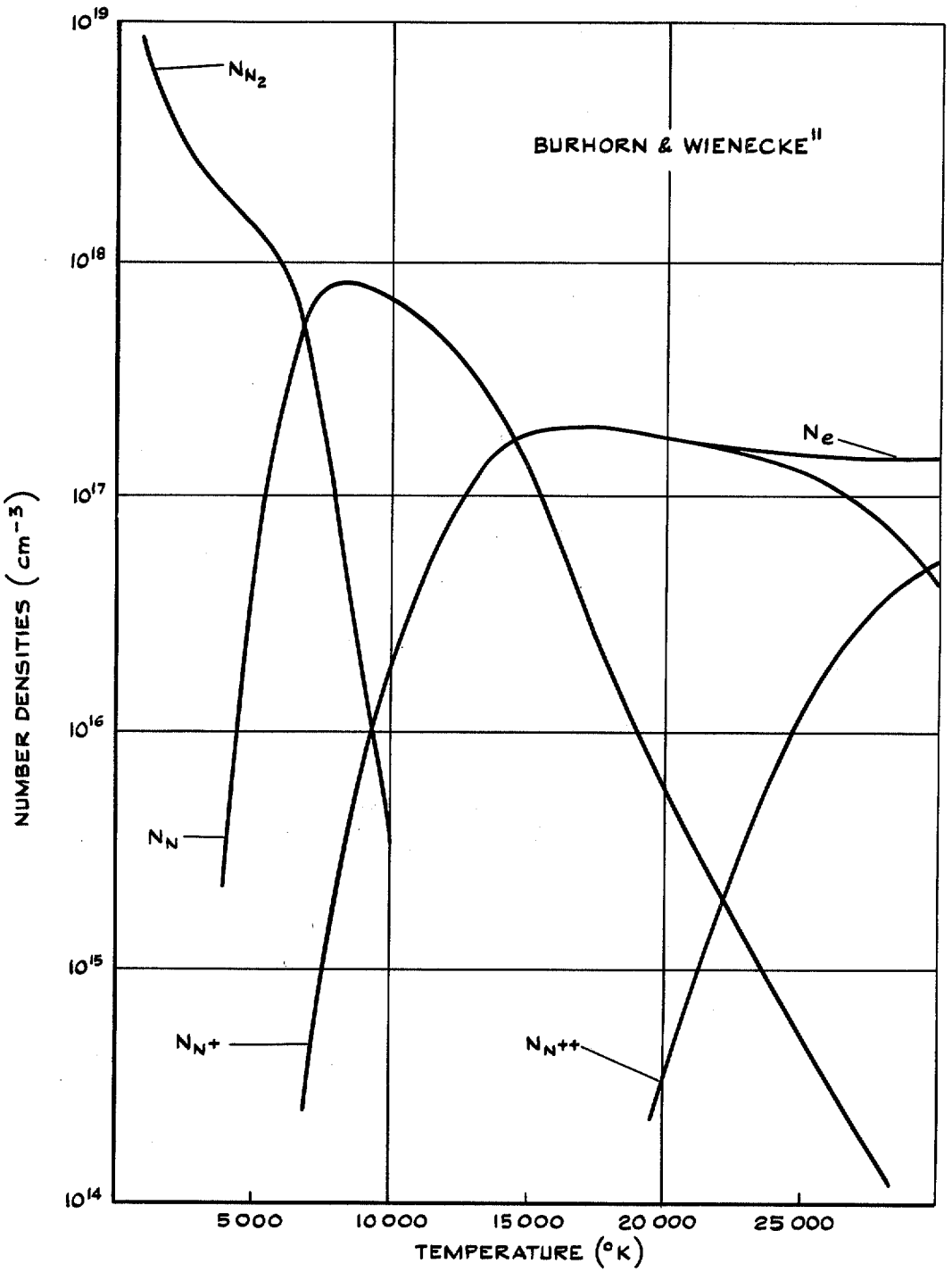


FIG. 11. Number densities of constituents of a nitrogen plasma at 1 atmosphere.

Printed in Wales for Her Majesty's Stationery Office by Allens Printers (Wales) Ltd.

Dd. 135646 K.5

Published by
HER MAJESTY'S STATIONERY OFFICE

To be purchased from
49 High Holborn, London W.C.1
13A Castle Street, Edinburgh 2
109 St. Mary Street, Cardiff CF1 1JW
Brazannose Street, Manchester M60 8AS
50 Fairfax Street, Bristol BS1 3DE
258 Broad Street, Birmingham 1
7 Linenhall Street, Belfast BT2 8AY
or through any bookseller


S. O. Code No. 23-3580